

## Influence of special plaster on the out-of-plane behavior of masonry walls

Mahmut Sami Donduren<sup>1</sup>, Recep Kani<sup>2</sup>, Ilker Kalkan<sup>3</sup> and Osman Gencil<sup>\*4</sup>

<sup>1</sup>Department of Civil Engineering, Faculty of Engineering, Selcuk University, 42075 Konya, Turkey

<sup>2</sup>Department of Civil Engineering, Faculty of Technology, Gazi University, 06500 Ankara, Turkey

<sup>3</sup>Department of Civil Engineering, Faculty of Engineering, Kirikkale University, 71450 Kirikkale, Turkey

<sup>4</sup>Department of Civil Engineering, Faculty of Engineering, Bartin University, 74100 Bartin, Turkey

(Received December 24, 2014, Revised December 7, 2015, Accepted December 16, 2015)

**Abstract.** The present study aimed at investigating the effect of a special plaster on the out-of-plane behavior of masonry walls. A reference specimen, plastered with conventional plaster, and a specimen plastered with a special plaster were tested under reversed cyclic lateral loading. The specimens were identical in dimensions and material properties. The special plaster contained an additive, which increased the adherence strength of the plaster to the wall. The amount of the additive in the mortar was adjusted based on the preliminary material tests. The influence of the plaster on the wall behavior was evaluated according to the initial cracking load, type of failure, energy absorption capacity (modulus of toughness), and crack pattern of the wall. Despite having limited contribution to the ductility, the special plaster increased the ultimate load capacity of the wall about 25%. The failure mode of the wall with special plaster resembled the plastic failure mechanism of a reinforced concrete slab in the formation of yielding lines along the wall. The deflection at failure and the modulus of toughness of the wall with special plaster were measured to be in order of 60% and 75% of the corresponding values of the reference wall.

**Keywords:** composite plaster; earthquake loading; plastered infill wall; out-of-plane behavior

### 1. Introduction

A majority of structures in the rural and semi-rural residential areas in developing and underdeveloped countries are made of masonry materials, such as clay bricks, mud bricks, natural shaped stones, cut stones and solid or hollow concrete blocks. These masonry units are bonded together with the help of different types of mortars, including mud mortar, cement-sand mortar and cement-sand-lime mortar. Masonry structures are more vulnerable to earthquake damage compared to concrete, steel and steel-concrete composite structures due to two main reasons:

1. Masonry structures are generally non-engineered structures, meaning that they are built in

---

\*Corresponding author, Associate Professor, E-mail: [ogencil@bartin.edu.tr](mailto:ogencil@bartin.edu.tr)

<sup>a</sup>Professor, E-mail: [rkanit@gazi.edu.tr](mailto:rkanit@gazi.edu.tr)

<sup>b</sup>Associate Professor, E-mail: [ilkerkalkan@kku.edu.tr](mailto:ilkerkalkan@kku.edu.tr)

<sup>c</sup>Associate Professor, E-mail: [sdonduren@selcuk.edu.tr](mailto:sdonduren@selcuk.edu.tr)

traditional ways with no assistance from engineers. Furthermore, most of these structures are built with poor workmanship.

2. Due to the use of low quality materials (masonry units and mortar), masonry structures possess significantly lower earthquake resistance than concrete and steel structures. Furthermore, most of these structures are not Unrecapable of behaving in a ductile manner during an earthquake as a result of the lack of a proper bond between the masonry units and mortar.

Masonry structures can be classified into three main groups: unreinforced masonry, confined masonry and reinforced masonry structures. Among these three groups, unreinforced masonry buildings constitute the conventional masonry system in the rural areas of many countries all around the globe. Due to their high vulnerability to earthquake damage, the use of unreinforced masonry system is not allowed in the zones of high seismicity in many countries. Nevertheless, unreinforced masonry buildings still constitute an important part of the building stock in the rural and semi-rural areas of the developing and underdeveloped countries. Therefore, the earthquake performance of unreinforced masonry structures and strengthening techniques for improving their earthquake performance is a significant subject of research.

Unreinforced masonry structures are composed of reinforced concrete slabs and roof, masonry walls and foundation. These structures are designed in a way that the vertical loads from the roof and the slabs are transmitted to the foundation through the walls. The horizontal ground accelerations induce lateral inertial forces in the floors and roof, where the majority of the building mass is present. These inertial forces need to be resisted by the masonry walls while transmitting them to the foundation. A ground motion in a specific direction causes certain walls of the building to be subjected to in-plane bending yet the remaining walls, which are subjected to forces along their thickness, undergo out-of-plane bending. Since the out-of-plane flexural rigidities of the walls are much smaller than their in-plane flexural rigidities, the walls experiencing out-of-plane bending are much more susceptible to failure under the earthquake-induced forces (Fig. 1). Consequently, the earthquake-resistant design of unreinforced masonry structures requires adequate connection between the walls so that the walls loaded in strong direction can support the walls loaded in weak direction.

Considering the lack of engineering assistance and quality control in the construction of masonry structures, structural integrity can generally not be achieved in unreinforced structural systems. For this reason, the masonry walls subjected to out-of-plane bending undergo brittle failure even in the case of moderate earthquakes. Previous researchers proposed and investigated different retrofit techniques to increase the out-of-plane flexural capacities and rigidities and to improve the ductilities of masonry walls. Ehsani *et al.* (1999) investigated the influence of externally-bonded vertical composite strips on the out-of-plane behavior of URM walls. The tests on three half-scale URM specimens indicated that this strengthening technique was capable of increasing the energy absorption capacity of an URM wall to a certain extent although both URM walls and composite strips have brittle stress-strain characteristics. The failure mode was seen to shift from delamination of the laminates to the tensile failure of the strengthened wall as wider and lighter laminates are used. Hamilton and Dolan (2001) tested six unreinforced concrete masonry walls under out-of-plane flexure and investigated the influence of GFRP composites containing unidirectional E-glass fabric on the out-of-plane behavior of URM walls. The composites were bonded to the wall in such a way that the fibers were oriented perpendicular to the bed joints of the wall. The composite was found to contribute to the flexural strength of the wall, significantly. Hamoush *et al.* (2001) used externally-bonded unidirectional and bidirectional woven glass and Kevlar fabric for strengthening URM walls and tested these walls under uniform out-of-plane



Fig. 1 Out-of-plane failure of URM walls (Kanit and Atimtay 2006)

loading. The tests indicated that concrete masonry unit (CMU) walls can reach their full flexural capacities only if the shear failure of the walls at the curtailment of the composite layers is prevented. Durham (2002) investigated the influence of using confining steel plates in the mortar joints on the in-plane flexural behavior of cantilever reinforced masonry walls with varying amounts of longitudinal reinforcement. The use of galvanized confining steel plates at every course within the plastic hinging region of the wall resulted in an increase about 90% in the displacement capacity of the wall. Ghobarah and El Mandooh Galal (2004) tested five full-scale unreinforced masonry (URM) block walls with different opening configurations, representing the windows and doors in URM buildings. The walls were subjected to cyclic out-of-plane loading. The CFRP laminates improved the out-of-plane bending capacities of the URM walls significantly and provided a better composite action between the mortar and the masonry units (concrete blocks). Kanit and Atimtay (2006) tested a masonry unit, composed of main wall and two additional wall segments orthogonal to the main wall, under reversed cyclic out-of-plane loading. This test indicated that the load transfer mechanism in a wall subjected to out-of-plane bending resembles the load transfer mechanism of a solid two-way slab. Accordingly, the lateral loads perpendicular to the plane of a wall are transmitted to the adjoining orthogonal walls and this load transfer results in a “complex pattern of cracking” in the wall, which resembles the yielding lines of a two-way reinforced concrete slab. Haddad *et al.* (2010) strengthened unreinforced concrete masonry walls on one side with sprayed GFRP and tested plain and strengthened walls under distributed loading, increasing from top to the bottom of the wall. The tests indicated that the thickness of the GFRP layer and the area covered with GFRP increase the ability of an URM wall to resist lateral load. Papanicolaou *et al.* (2011) used externally bonded grids for strengthening perforated clay brick and solid stone masonry walls and conducted experiments on medium-scale wall specimens in either a combination of in-plane flexure and axial force or a combination of out-of-plane flexure, in-plane shear and axial force. Different types of grids and bonding agents proved to be efficient in upgrading the in-plane and out-of-plane flexural behavior of existing masonry

structures.

Dizhur *et al.* (2010a, b, c) conducted laboratory and in-situ experiments on clay brick masonry walls under uniform out-of-plane loading. The near-surface mounted (NSM) CFRP strips greatly contributed to the flexural capacities and ductilities of URM walls. In all walls, the final failure resulted from debonding of the CFRP strips or shear failure of the wall and in none of the walls the strips reached their full axial tensile capacities. Ismail *et al.* (2011) investigated the influence of retrofitting with post-tensioned threaded bars and seven-wire strands on the out-of-plane flexural behavior of clay-brick URM walls, constructed with salvaged material from an old URM structure. In all strengthened specimens, the post-tensioning bar and strands extended through the entire height and located at the center (mid-length) of the wall. The post-tensioning bars and strands were able to limit the width of a main crack initiating at mid-height of the wall due to the plastic hinging at this location. Unlike the single threaded bar, which yielded during the test, the wire strands were capable of providing the walls with a nonlinear elastic behavior, which was considered as an advantage for the immediate use of a structure after the earthquake. Babaeidarabad *et al.* (2014) found out that fabric-reinforced cementitious matrix (FRCM) effectively improves the flexural capacities and stiffnesses of clay brick walls under out-of-plane loading, simulating high wind pressures and earthquakes. Increasing amounts of FRCM resulted in considerable increase in the out-of-plane capacities of the walls. Babaeidarabad and Nanni (2015) applied two different amounts of FRCM reinforcement (1-ply and 4-ply) for strengthening concrete block and clay brick masonry walls. Each FRCM ply was composed of two layers of cementitious mortar and a ply of carbon fabric between them. The test results indicated that the application of 1-ply strengthening layer shifted the failure mode to the rupture of the fabric and increased the load capacities of the URM walls to about 3 times the capacities of the respective control walls. Application of the 4-ply strengthening layer, on the other hand, shifted the failure mode to shear failure as a result of the high flexural capacities of the strengthened walls and increased the ultimate load values to about 9 times the respective capacities of the respective control walls. Similar to the improvement in the behavior of clay brick walls, Prota *et al.* (2006) found out that cementitious matrix-grid composites, particularly the cement based matrix-coated alkali resistant glass grid system (CMG), effectively improved the in-plane diagonal compression behavior of the tuff masonry panels, representing the historical tuff buildings in the Mediterranean region. Augenti *et al.* (2011) established the efficiency of the inorganic (cementitious) matrix-grid composites in repairing the in-plane flexural behavior of URM walls. De Felice *et al.* (2014) presented the results of the unidirectional tensile tests and strengthening layer-to-masonry bond strength tests of mortar-based composite materials. The mechanical properties of steel reinforced grouts, carbon textile reinforced mortars and basalt textile reinforced mortars were examined based on the results of an extensive research program conducted in three different European universities in an effort to increase the efficiency of the use of these materials for improving the earthquake behavior of brick and stone masonry structures. Basaran *et al.* (2015) investigated the contribution of polypropylene and steel fibers in the plaster to the diagonal tensile capacities of blend brick walls. The experimental and numerical studies indicated that the load-deflection behavior of these walls under diagonal loads can be improved by the addition of fibers to the plaster.

Although promising results were obtained by previous researchers for improving the in-plane and out-of-plane flexural behavior of URM walls, the investigated methods require significant amount of time and labor for retrofitting all of the walls of a building. Considering the fact that a great majority of the buildings in the rural areas are URM structures, the application of the proposed retrofit techniques to all of these structures become cumbersome, if not impossible. In

the present study, a quite simple retrofit technique for URM buildings was proposed. The study of Kanit and Atimtay (2006) indicated that the cracks, initiating at the masonry units and mortar, propagate and form failure lines, which in turn result in the complete failure of the wall. Accordingly, the complete failure of a wall can be delayed if the initiation and propagation of the cracks in the plastered wall can be impeded. In the present method, a special type of mortar, whose bond strength to masonry was improved through the use of an additive, was used to delay the formation of cracks in the wall. In this way, the out-of-plane flexural behavior of the wall was intended to be improved by increasing the deformation capacity of the plastered wall. Preliminary tests were conducted on wall samples to determine the optimum amount of additive to increase the bond strength of the mortar to the wall. After these preliminary tests, two URM specimens, each composed of a main wall and two orthogonal wall segments, were tested to failure. The main wall was subjected to reversed cyclic out-of-plane loading, simulating the horizontal ground motions. The influence of the special mortar on the out-of-plane flexural behavior of URM walls was evaluated based on the load capacity, stiffness and energy absorption capacity of the wall.

## **2. Experimental study**

The present experimental program was carried out to investigate the influence of a special type of mortar on the out-of-plane flexural behavior of unreinforced clay brick walls. The mortar contained a special additive, SikaLatex, which increases the adhesion property and water resistance of the mortar. By the use of this additive, the initiation and propagation of the cracks in the wall, which eventually lead to the failure of the wall by forming failure lines, was aimed to be delayed. The out-of-plane flexural capacity of the wall was assumed to increase and the out-of-plane behavior to improve due to the delay in the formation of failure lines.

### *2.1 Preliminary experiments*

The optimum amount of the additive for providing the mortar with the greatest bond strength to masonry was determined with the help of preliminary tests. In these tests, six wall samples with dimensions of 600×600×200 mm were subjected to monotonic diagonal loading (Fig. 2). The mortar mixture, used in each specimen, was also used for plastering both faces of the wall. The mixing proportions of mortar are tabulated in Table 1 for each specimen.

In these tests, the specimens were loaded with the help of loading shoes, which confined the upper and lower corners of the wall similar to the test procedure summarized in ASTM E519 (ASTM 2010). As shown in Fig. 2, a steel angle was placed on each of the loaded corners of the wall and the loading shoes were seated on these angles. The gaps between the angles and the loading shoes were filled with plaster. This plaster was used for preventing the gap from affecting the load and deflection measurements until the loading shoes come in contact with the angles. The specimens were placed in the test setup with the help of plumb line to ensure concentric loading. The wall was allowed to deform only in plane with the help of a lateral bracing system, illustrated in Fig. 2. The arms of the lateral bracing system in contact with the specimen were oiled before each test to prevent any restraint to the in-plane deformations of the wall. The load was applied by a hydraulic jack and measured with the help of an electronic load cell, each having a capacity of 500 kN. An additional plate was placed between the upper loading shoe and the hydraulic jack to adjust the level of the jack before the test.

Table 1 Mixing proportions of mortar in weight

Specimen	Sikalatex (kg)	Water (kg)	Cement (kg)	Sand (kg)
1	0.5	1.5	2.5	8
2	0.75	0.75	3	10
3	1.2	0.6	4	9
4	2.6	1.6	7.5	15
5	3	1.2	7.5	15
6	3.5	1	7.5	15

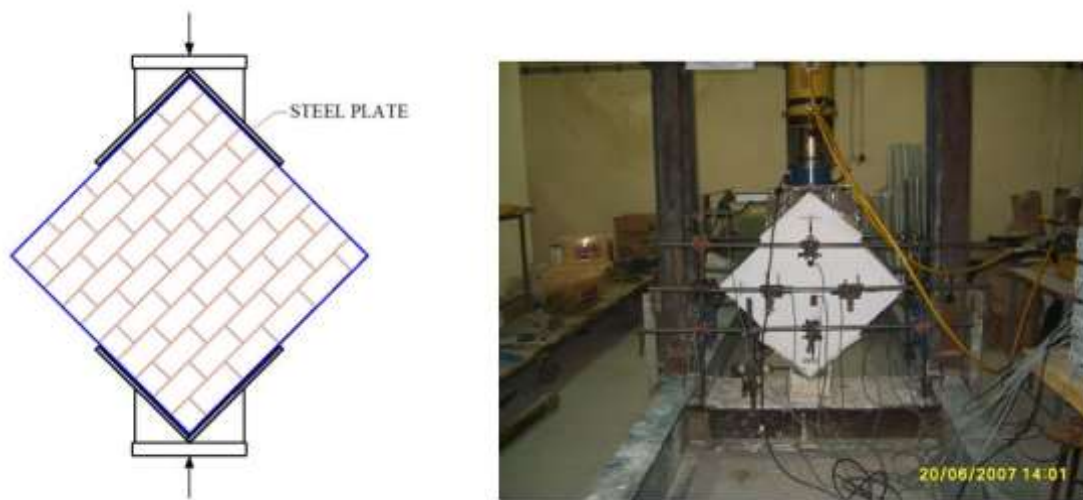


Fig. 2 Preliminary experiments

Ten different LVDT's were used for measuring the deformations of the specimens at different locations (Fig. 3). The shortening along the loaded diagonal was measured with the help of four LVDT's, two on each of the front and back faces of the wall. The elongation along the diagonal perpendicular to the loaded one was measured with the help of four transducers, two on each of the front and back faces of the specimen.

Finally, two additional transducers were used for controlling the out-of-plane movement of the wall during the test. Based on the measurements from these two transducers, loading could be stopped if out-of-plane bending moments arised in the tests due to any accidental eccentricities in the applied load and the lateral restraining system was not capable of preventing these out-of-plane translations. The transducers had a precision of 0.01 mm.

The specimens were tested to failure (Fig. 4). The load-deflection curves of the specimens are illustrated in Fig. 5. Among the specimens, the third specimen reached the greatest ultimate load and had the greatest initial rigidity. Table 2 summarizes the results of the preliminary experiments. The ultimate loads of the other specimens can be seen to be smaller than the load capacity of specimen 3 between 11-50%. Similarly, the initial rigidity of specimen 3, which is calculated from the ratio of the cracking load to the displacement at the onset of cracking, was greater than the respective values of the remaining specimens in the range of 43-63%. Finally, the table also

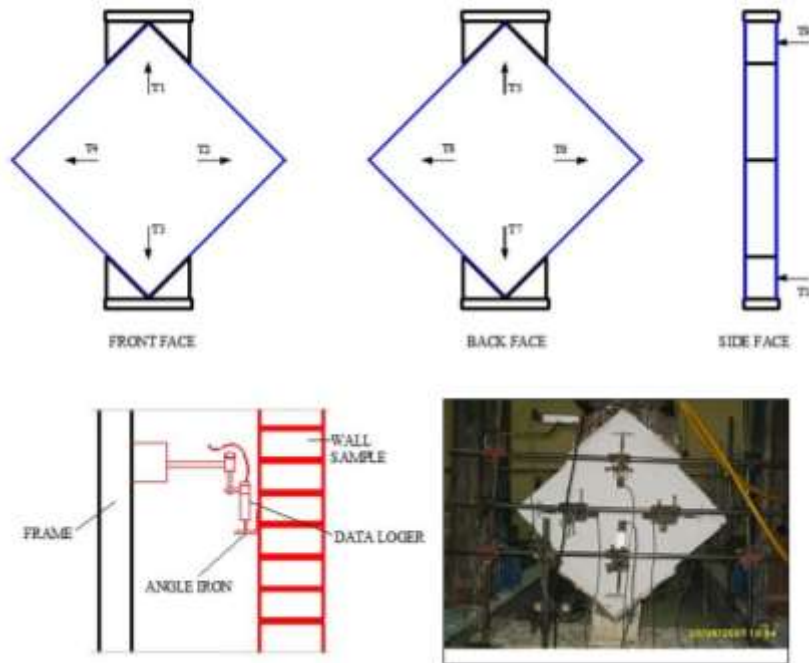


Fig. 3 Measurement system used in the preliminary experiments



Fig. 4 Failure of specimen 3

presents the deformation ductility index values of the specimens. In the present study, the deformation ductility index was calculated from the ratio of the deflection at ultimate load to the deflection at cracking load. The tails of the load-deflection curves were not considered in the calculation of ductility index since the specimens failed very suddenly after reaching the peak load.

The index values indicate that the ductility of specimen 3 was smaller than the ductility values of three of the specimens by only 5-20%. Although the ductility of specimen 3 remained below some of the other specimens, the mix proportions of specimen 3 (Table 1) were adopted in the main tests due to the significantly higher load capacity and initial rigidity values of this specimen. As observed in Fig. 4, the specimens tested in the preliminary study mostly failed due to diagonal tension cracking along the loaded diagonal, which was also triggered by the high stress concentrations in the loaded corners.

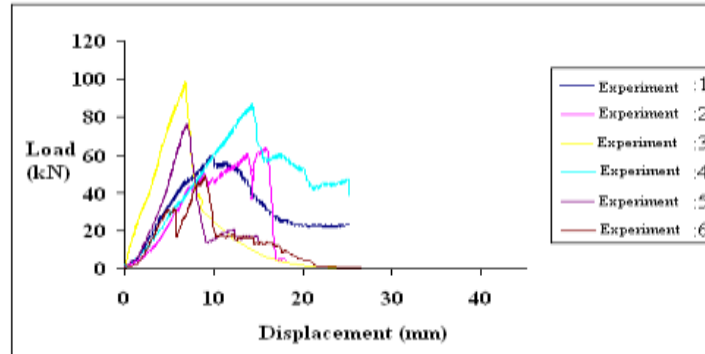


Fig. 5 Load-deflection curves of the specimens

Table 2 Results of the preliminary experiments

Test	Ultimate Load		Initial Rigidity		Ductility	
	Value (kN)	% Diff. from Spe. 3	Value (kN/mm)	% Diff. from Spe. 3	Value	% Diff. from Spe. 3
1	59.7	-39	5,3	-63	2,1	10
2	63.6	-35	5,9	-59	2,3	20
3	98.2	0	14,3	0	1,9	0
4	75.5	-23	5,7	-60	2,0	5
5	87.1	-11	8,2	-43	1,5	-22
6	49.6	-50	6,4	-55	1,9	0

## 2.2 Specimens of the main stage of the experimental program

Two full-scale URM specimens, made up of 190×190×50 mm solid blend bricks, were tested to failure. The first specimen, denoted as the reference wall (RW), was constructed using regular mortar, while a special type of mortar including the additive Sikalatex was used in the second specimen, denoted as the model wall (MW). The mixing proportions of the mortar used in MW were identical to the proportions of the mortar in the third specimen, tested in the preliminary stage of the experimental program. The mixing proportions of the mortar in RW and MW are illustrated in Table 3.

The two specimens only differed in the mortar mixture. The specimens were composed of a main wall, two additional wall segments in perpendicular direction to the main wall, a reinforced concrete slab and three lintel beams, one on each wall. The main wall had a length of 2600 mm and an overall height of 2600 mm. Each of the perpendicular wall segments had a length of 1100 mm and an overall height of 2600 mm. Each face of the wall was covered with a 20-mm thick coarse and 10-mm thick fine plaster.

The blend bricks were laid in alternative courses of headers and stretchers (Fig. 6(a)). Each brick was cleaned with compressed air before bricklaying. The mortar joints between the bricks had a uniform thickness of 20 mm throughout the specimen. After completion of bricklaying, formwork of the slab and lintel beams was assembled, reinforcement was laid (Fig. 6(b)) and concrete was cast into the forms. Later, the walls were plastered (Fig. 6(c)) with the mortar

mixture presented in Table 3. After moist-curing of the plaster and concrete for seven days, the plaster was left to dry for three more days. Finally, the walls were limewashed to make the cracks more visible during the tests (Fig. 6(d)).

Six brick specimens of 70×95×100 mm, cut from the blend bricks, were tested to failure under uniaxial compression based on the British Standards BS EN 772-1:2000 (BS 2000). The specimens had an average compressive strength of 23.2 MPa with a coefficient of variation of 9.5%. The material tests also indicated that the brick had an average modulus of elasticity of 3000 MPa. Three samples taken from each of the M8 and M12 bars were tested under uniaxial tension. The M8 and M12 bars used in the specimens had average yield strength values of 450 and 480 MPa with standard deviation values of 15 and 35 MPa, respectively. The M8 and M12 bars had average ultimate strength values of 600 and 610 MPa with standard deviation values of 15 and 40 MPa, respectively. Finally, the average percent elongation values of M8 and M12 bars were measured as 18 and 20 with standard deviation values of 1.70×175 mm cylinder specimens were tested under axial compression to determine these compressive strength values. Three cylinders were taken from each of the mortar mixtures of specimen RW and MW. The material tests indicated that the mortar mixtures of RW and MW had mean compressive strength values of 6.6 MPa and 8.5 MPa with standard deviation values 0.3 and 0.6 MPa, respectively. Since the compressive strength values of these two mixtures are quite close to each other, the differences between the experimental results of RW and MW can mostly be attributed to the influence of the special additive to the bond strength of the mortar to the wall, rather than the compressive strength of the plastered wall.

Each of the fine and coarse plaster layers of each specimen (RW and MW) was prepared as a single batch for uniformity throughout the specimen. Prior to the application of the plaster layers, wooden planks extending throughout the wall height were installed on each corner of the specimen (Fig. 6(c)) to adjust the thickness of the plaster layer. After the application of plaster, the plaster surface was leveled with a long screed board, which also provided the plaster with uniform thickness along the wall.

### 2.3 Test setup and test procedure

The test setup illustrated in Fig. 7 was used for applying reversed cyclic out-of-plane loading to the main wall of each specimen. The load was applied by a double action hydraulic jack, connected to a reaction wall (Fig. 8). A steel rod, fixed to the hydraulic cylinder at one end, was welded to a steel plate on the front (exterior) face of the wall (Fig. 9). This plate was connected to another steel plate, located on the interior face of the wall. The exterior and interior plates were connected to each other with the help of four bolts at the corners of the plates. Both the exterior and interior plates were centered on the wall. The bolts, passing through the wall, and the plates were used for applying reversed loading to the wall. Epoxy was injected to the bolt holes before installation of the loading plates to prevent the formation of weak zones in the wall. The presence

Table 3 Mixing proportions of mortar in the main stage of the experimental program

Specimen	Sikalatex (kg)	Water (kg)	Cement (kg)	Sand (kg)
RW	-	1.8	4	9
MW	1.2	0.6	4	9

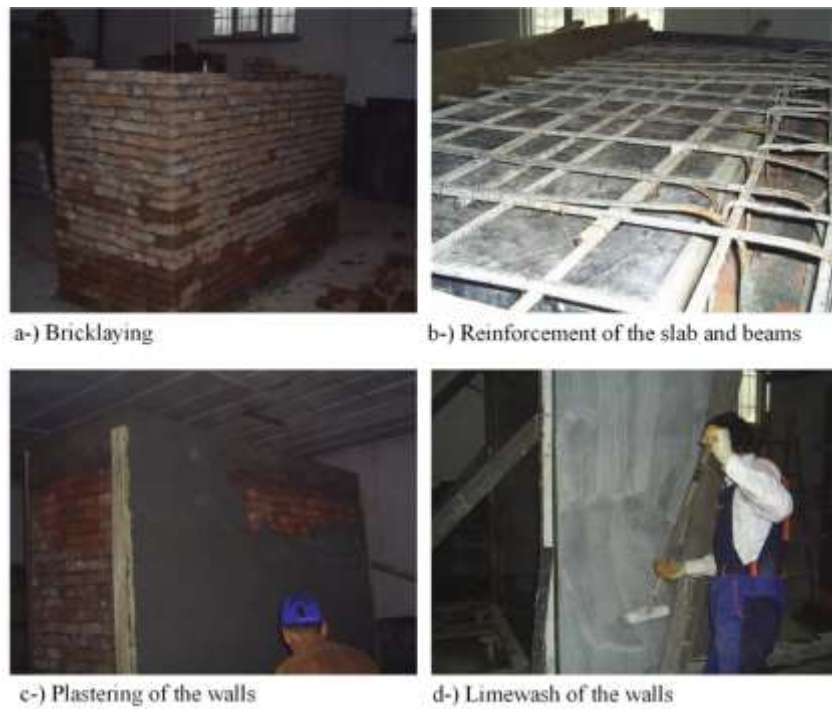


Fig. 6 Construction of test specimens

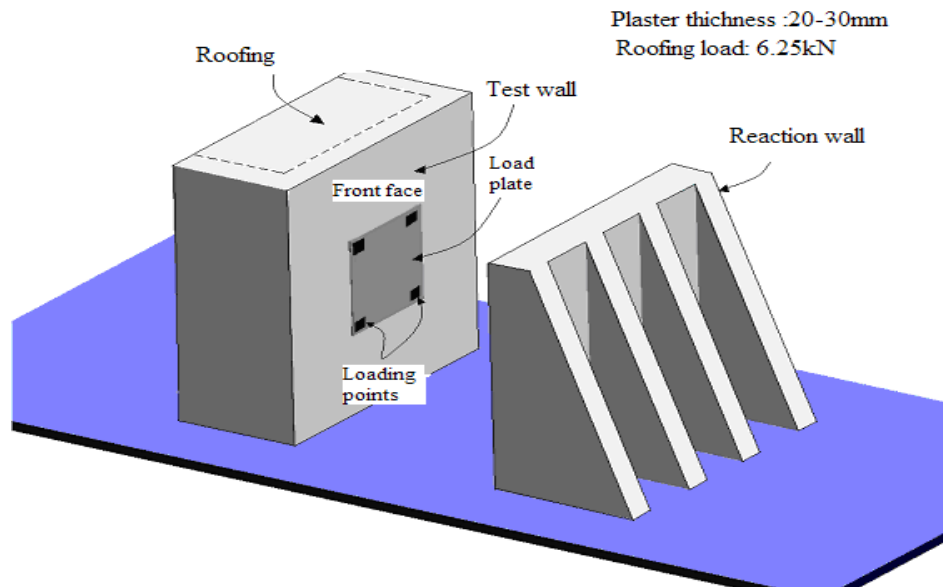


Fig. 7 The test setup

of four small holes in the wall instead of a large hole at the center of the wall (single concentrated loading at the center) was adopted since a large hole would have more detrimental effects on the

wall behavior compared to small holes. The locations of the bolt holes were chosen to be on the expected failure lines of the walls so that these holes have minimal influence on the wall behavior. The weights of the plates were supported with the help of wooden frames (Fig. 8) so that the plates do not apply too much pressure to the bolts and the wall.

With the help of the loading plates, the applied load was divided into four point loads, yielding to a moment diagram similar to the one created by uniform distributed out-of-plane loading throughout the wall. This loading scheme simulates the effects of a lateral ground acceleration on a wall subject to weak-axis bending. A total vertical load of 6.25 kN was also applied to the test

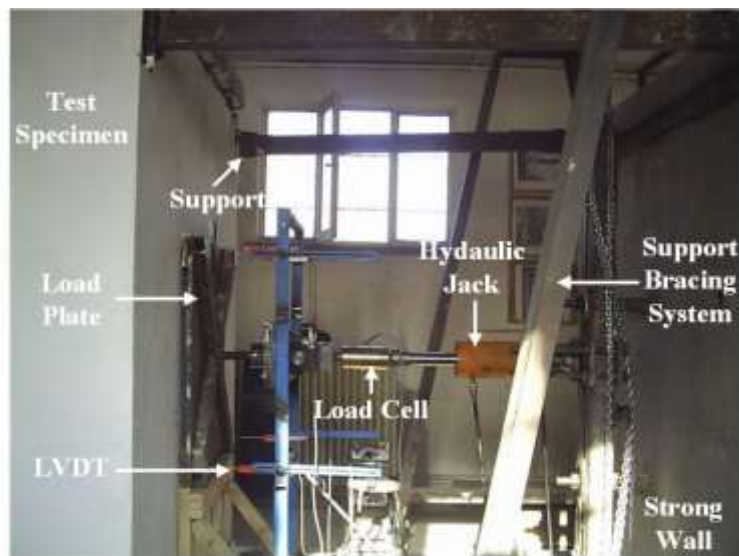


Fig. 8 The loading and support rigs



Fig. 9 The loading mechanism

specimen with the help of concrete blocks, placed on the slab. This surcharge represents the equivalent distributed load on the main wall induced by the uniform design live load of the slab of a residential structure, which is given as  $2 \text{ kN/m}^2$  in the Turkish Standard TS 498 (TS 1997). The plan dimensions of the prototype structure between the center lines of the walls were taken  $2350 \times 1950 \text{ mm}$  in the calculation of this surcharge value.

The main wall was restrained from out-of-plane translation at the upper and lower corners with the help of a support mechanism (Fig. 8). To ensure that the corners of the wall are prevented from out-of-plane deflections, a second support system was used to support the upper and lower ends of the perpendicular wall segments in addition to the support system, connected to the corners of the main wall.

The lateral deflections of the wall were measured with the help of electronic LVDT's, having strokes of 100 and 200 mm. Each LVDT had a precision of 0.01 mm. A total of 9 transducers were used for measuring the deflections at four loading points (Fig. 8), at the center of the plate and at the upper and lower corners of the wall. The load was measured with the help of a load cell, connected to the jack (Fig. 8). The load and deflection measurements were constantly monitored and recorded through a DAQ system and computer.

The specimens were subjected to reversed cyclic out-of-plane loading in two different load increments throughout the test. Up to a load value of 40 kN, a load increment of 10 kN was adopted, while a load increment 5 kN was used beyond this load. After reaching the ultimate load, the applied load was decreased at a load increment of 5 kN. A smaller load increment was adopted beyond 40 kN so that the damage state and propagation of cracks in the walls could be observed more clearly and more frequently beyond cracking load.

#### *2.4 Evaluation of the test results*

The lateral deflections of the specimens at the center of the wall were calculated from the average of the deflection measurements of the four transducers at the corners of the load plate. The deflections resulting in compression at the exterior (front) face and tension at the interior (back) face of the main wall at midspan were accepted as positive and the loading in this direction was denoted as forward loading. The crack patterns and damage states of RW and MW are illustrated in Fig. 10 and Fig. 11, respectively. Furthermore, the load-deflection graphs of the two specimens are shown in Fig. 12 and Fig. 13. In these figures, the deflections at the center of the wall, measured at the inner and outer faces of the main wall, are illustrated.

The reference specimen RW failed in a brittle manner at an ultimate load value of 65 kN in both forward and reverse cycles of loading. The initial cracks formed around the center of main wall and in the perpendicular wall segments at an applied load of 40 kN in the forward cycle of loading. This value is very close to the analytical cracking load of RW, which is calculated by assuming that the wall is a flexural member with a cross-section of  $2100 \times 250 \text{ mm}$  and a length of 2350 mm (the distance between the centerlines of the perpendicular wall segments), subjected to weak axis bending. The analytical cracking load can be calculated as 43 kN, assuming that the tensile strength of plaster is 0.1 times its compressive strength (6.6 MPa). After initiation of cracking, the rigidity of the wall decreased at about 50% of its precracking rigidity and the natural period of the specimen increased to about 1.40 times its initial period. This decrease was calculated from the acceleration response spectrum given in the Turkish Earthquake Code (TEC 2007), by assuming that the out-of-plane acceleration acting on the main wall dropped to 50% of its pre-cracking value after the initiation of cracking in the wall. Specimen RW exhibited very

limited ductility after reaching the ultimate load. As shown in the final state (Fig. 10) and crack pattern (Fig. 14) of RW, diagonal cracks propagating from the loading points to the corners of the main wall formed at the front (exterior) face of the wall, while horizontal cracks extending between the two supports formed on the back (interior) face of the wall. In addition to the cracks in the main wall, diagonal and horizontal cracks formed in the perpendicular wall segments. The cracks widths were measured to be around 20 mm at failure.

The major damage in specimen RW formed on the exterior faces of the main wall and the perpendicular wall segments, indicating that the damage was caused by the forward direction of loading. A number of cracks, which formed parallel to the exterior edges of the main wall in the perpendicular wall segments, indicate that considerable stresses developed at the intersections of the walls. The crack pattern on the exterior face of the main wall (Fig. 14(a)) resembles the yield lines of a two-way reinforced concrete slab. This crack pattern implies that the load transfer from the center of the main wall to the supporting perpendicular walls is similar to the transfer of the loads from a two-way slab to the surrounding beams.

The wall MW with special mortar, on the other hand, reached a higher ultimate load (80 kN) in the forward cycle compared to RW. In other words, the additive SikaLatex increased the load capacity of the wall in the forward direction at about 20%. As shown in Fig. 13, the ultimate load of RW in the backward direction of loading is measured to be around 60 kN, implying that the additive had little or no influence on the load capacity of the wall in the reverse direction of loading.

In MW, the first crack, which was a very thin crack extending from the left support to the load plate on the exterior face, formed at a load level of 55 kN. This experimental cracking load is close to the analytical cracking load value of 55 kN. The rigidity of MW decreased to about 60% of its precracking rigidity after the initiation of cracking. The smaller decrease in the rigidity of MW due to the initiation of cracking indicates the contribution of the additive to the rigidity of the specimen after the formation of tension cracks in the plastered wall. As shown in Figs. 11 and 14, horizontal



Fig. 10 The final state of RW



Fig. 11 The final state of MW

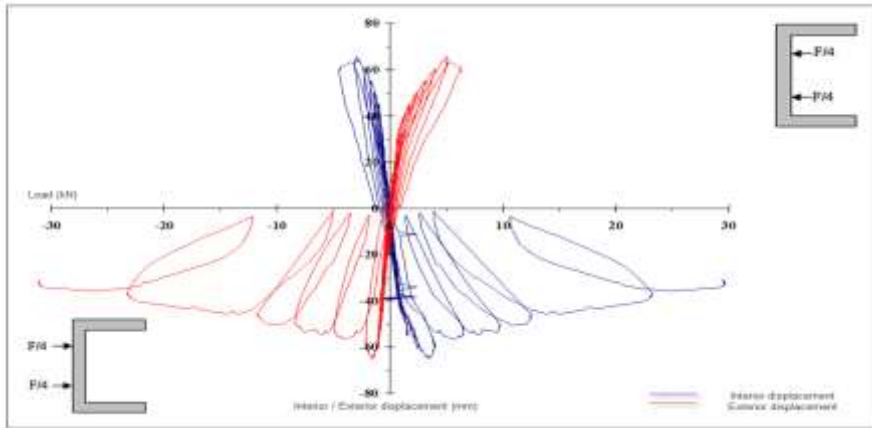


Fig. 12 The load-deflection curve RW

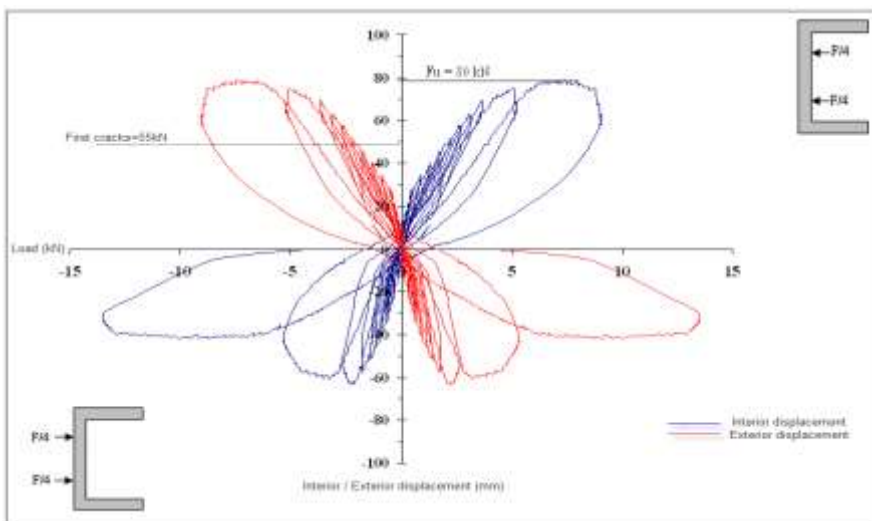


Fig. 13 The load-deflection curve MW

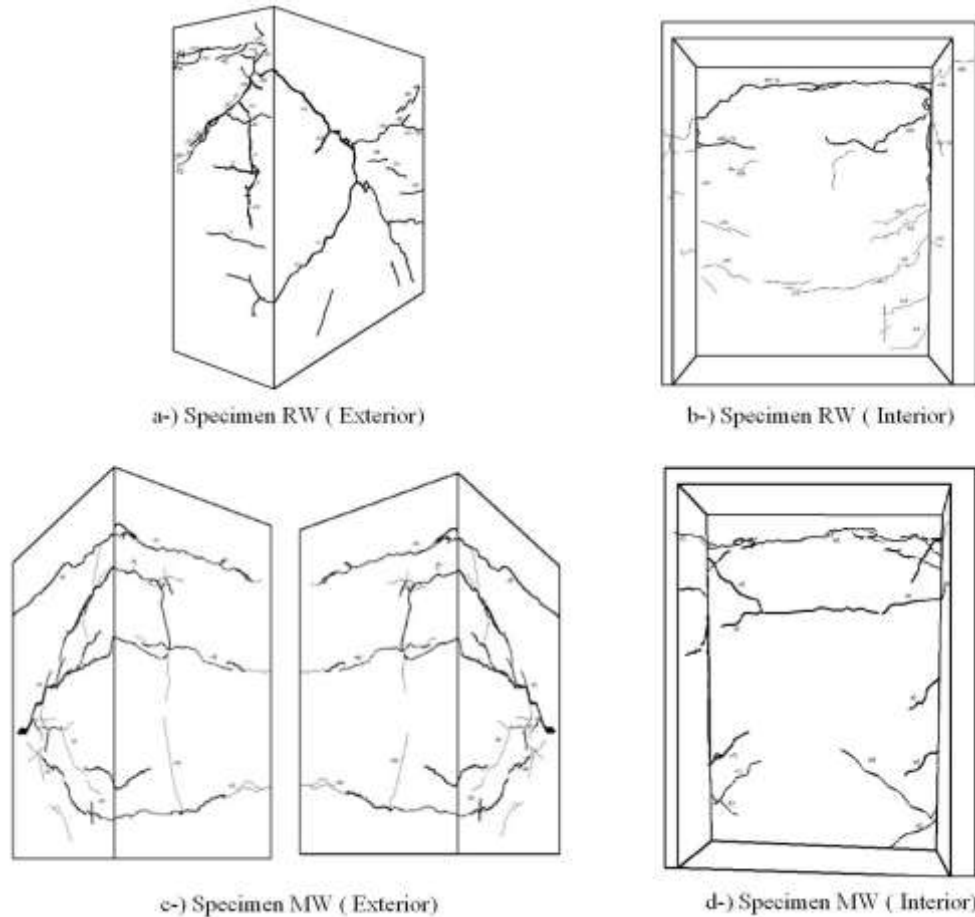


Fig. 14 Crack patterns of the specimens at failure

cracks extending from the edges to the load plate and diagonal cracks extending from the loading points to the corners of the wall formed on the front (exterior) face of the main wall.

Similar to specimen RW, horizontal cracks extending between the two supports formed on the interior face of specimen MW. The cracks extending from the center of the wall to the edges and corners continued along the perpendicular wall segments as horizontal and diagonal cracks (Fig. 14(c)). Similar to specimen RW, the major cracks in MW formed on the exterior faces of the specimen under the forward direction of loading.

The modulus of toughness values of specimens RW and MW were calculated as 1080 and 750 kN.mm, respectively. These values were calculated from the area under the envelope load-deflection curves of specimens corresponding to the interior displacement in the reverse direction of loading. The reverse direction of loading was used for the calculation of the modulus of toughness values since the main wall underwent greater displacements in the reverse direction and the final failure of the specimens took place in this direction (Figs. 12 and 13). That's why, the deformations of the main wall in the reverse direction are of greater importance and this direction

of loading should be considered for evaluating the deformability of the specimen out of plane. In contrast to the expectations, the additive did not contribute to the energy absorption capacity of the wall under out-of-plane loading. Accordingly, this special plaster increases the load capacity, the cracking load and the post-cracking rigidity of an URM wall, while having no contribution to its energy absorption capacity under out-of-plane bending.

The same conclusion can be drawn from the total absorbed energy versus load cycle relationships of the specimens, illustrated in Fig. 15. Throughout the entire course of loading, specimen RW can be seen to have absorbed greater energy compared to specimen MW. The smaller absorbed energy values of specimen MW stem from the fact that MW underwent smaller deformations than specimen RW due to its greater rigidity. Consequently, the area under the load-deflection curve of MW was smaller than the respective area of RW per each hysteresis cycle, since RW experienced plastic deformations in cycles, which resulted in only elastic deformations in MW.

Previously, Erdal (2010) tested an URM specimens with identical components and dimensions to the specimens of the present study. In the study of Erdal (2010), a central FRP strip was applied to the outer face of the main wall of one of the specimens and a second plain specimen was tested as reference. The unidirectional CFRP strip had a thickness of 0.2 mm and width of 300 mm. As well as bonding the strip to the wall with epoxy, five steel plates at equal spacing were bolted to the wall along the height of the strip to prevent peeling-off of the strip. Erdal (2010) only applied an FRP strip to the outer surface of the wall for two reasons: 1-) The main wall is prone to fail out of plane when the loading creates tensile stresses at the outer surface of the main wall (reverse direction of loading). A similar conclusion was drawn in the present study. Figs. 12 and 13 indicate that the walls are liable to failure under forces creating tension at the outer face and compression at the inner face of the wall. 2-) Application of the strip to the outer surface will cause minimum disturbance to the occupants of the structure during strengthening process.

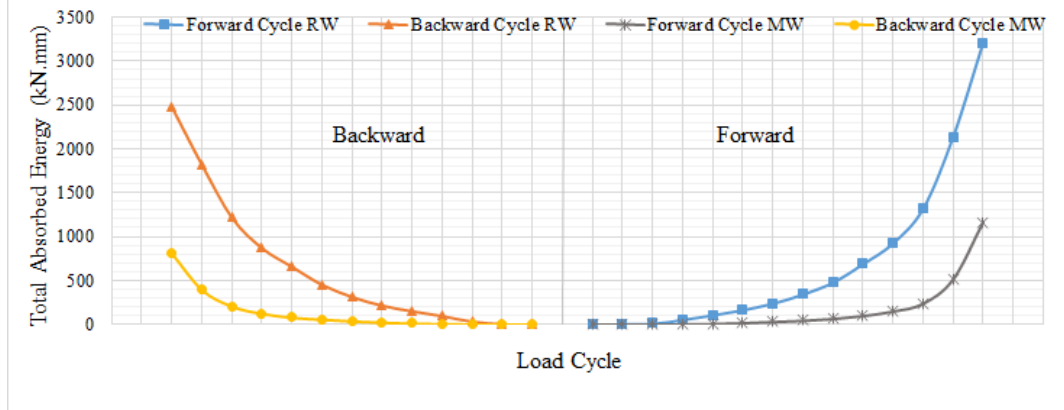
The strengthened specimen of Erdal (2010) failed at an applied load of 115 kN, corresponding to an increase of 75% in the load capacity with respect to the reference specimen (Fig. 16). Although the strengthening method of Erdal (2010) resulted in a much higher increase in the load capacity of the wall compared to the present strengthening technique, the present method bares several advantages over the use of FRP, including but not limited to economy, ease of application and the need for a reduced time and effort for the application of the special mortar to the wall. The method of Erdal (2010) also resulted in higher increases in the cracking load (80 kN) and the energy absorption capacity of the wall.

### **3. Conclusions**

The present paper summarizes an experimental study dedicated to investigate the influence of a special type of mortar on the reversed cyclic out-of-plane bending behavior of URM walls. The mortar contains an additive (Sikalatex), which increases the bond strength of the mortar to masonry. This additive was assumed to retard the formation of the tension cracks in the wall, and therefore, increase the deformations of the wall before complete failure. The study was composed of two stages. In the preliminary stage, six 600×600×200 mm URM assemblies were tested under monotonic diagonal loading to determine the optimum proportion of the additive that yields to the greatest bond strength.

In the main stage, two full-scale URM specimens, each composed of a main wall, two

perpendicular wall segments, a reinforced concrete slab and three lintel beams, were tested to



The two specimens were identical in dimensions and material properties and they only differed in the mortar mixture. In the reference specimen, the mortar and plaster did not contain any additive, while in the second specimen, the plaster and mortar contained the special additive, whose proportion was determined in the preliminary stage. This experimental study yielded to the following conclusions:

- The addition of the additive to the mortar mixture contributes to the load capacity and post-cracking rigidity of an URM wall subject to out-of-plane loading. Furthermore, the additive also retards the formation of the cracks in the wall. Nevertheless, the additive was not found to have any positive effect on the energy absorption capacity and deformability of URM walls and the energy absorbed by the wall per each load cycle.

- The exterior faces of URM walls were found to be prone to heavier damage than the interior faces. Accordingly, URM walls under reversed cyclic out-of-plane loading are generally expected to collapse towards the outside.

- The cracks in an URM wall under out-of-plane bending extend along the neighboring perpendicular walls due to the rotational and translational restraint provided by these walls. The presence of diagonal cracks as well as the vertical cracks in the perpendicular neighbor walls indicates that the perpendicular walls are under shear forces as well as bending moments.

- The additive does not reduce the tendency of an URM wall in weak-axis bending to separate from the neighboring support walls. Vertical cracks parallel to the edges of the main wall form near the interfaces between the neighboring walls whether the additive is used in the mortar mixture, or not.

- The present strengthening method cannot increase the load capacity and energy absorption capacity of an URM specimen as much as strengthening the main wall with FRP materials, if the materials are adequately bonded to the wall. Nevertheless, the present method requires much less effort and time and is much less costly compared to strengthening practices with FRP materials.

The above conclusions were drawn based on the test results of two specimens. Further experiments are needed to draw more general and exact conclusions, considering the normal variability in the masonry test specimens. The present study only focused on the out-of-plane behavior of URM walls, made up of blend bricks. Further studies are needed to investigate the influence of this additive to the in-plane behavior of URM walls and the effects of this additive on URM walls made up of different types of masonry units (stone, mud bricks, etc.).

## **Acknowledgements**

The study was funded by the Scientific Research Projects Coordinatorship of Selçuk University, Konya, Turkey with the project number 06401066. This funding is gratefully acknowledged. The material tests of the present study were carried out in the Structural Mechanics Laboratory of the Faculty of Engineering, Gazi University, Ankara, Turkey. The preliminary tests were conducted in the Earthquake Research Laboratory of the Faculty of Engineering, Selçuk University, Konya, Turkey. Finally, the main experiments were conducted in the Earthquake Research Laboratory of the Faculty of Technology, Gazi University, Ankara, Turkey.

## **References**

- ASTM E519/E519M-10 (2010), *Standard Test Method for Diagonal Tension (shear) in Masonry Assemblages*, American Society for Testing and Materials, West Conshocken, Pennsylvania, USA.
- Augenti, N., Parisi, F., Prota, A. and Manfredi, G. (2011), "In-plane lateral response of a full-scale masonry subassembly with and without an inorganic matrix-grid strengthening system", *J. Compos. Constr.*, **15**(4), 578-590.
- Babaeidarabad, S., Caso, F. and Nanni, A. (2014), "Out-of-plane behavior of URM walls strengthened with fabric-reinforced cementitious matrix composite", *J. Compos. Constr.*, **18**(4), doi: 10.1061/(ASCE)CC.1943-5614.0000457.
- Babaeidarabad, S. and Nanni, A. (2015), "Out-of-plane strengthening of URM walls with Fabric-Reinforced-Cementitious-Matrix (FRCM)", *ACI Spec. Pub.*, **299**, 1-12.
- Basaran, H., Demira, A., Bagci, M. and Ergun, S. (2015), "Experimental and numerical investigation of walls strengthened with fiber plaster", *Struct. Eng. Mech.*, **56**(2), 189-200.
- BS EN 772-1:2000 (2000), *Methods of Test for Masonry Units. Determination of compressive strength*, British Standards Institute, London, UK.
- De Felice, G., De Santis, S., Garmendia, L., Ghiassi, B., Larrinaga, P., Lourenço, P.B., Oliveira, D.V., Paolacci, F. and Papanicolaou, C.G. (2014), "Mortar-based systems for externally bonded strengthening of masonry", *Mater. Struct.*, **47**(12), 2021-2037.
- Dizhur, D., Derakhshan, H., Lumantarna, R., Griffith, M. and Ingham, J. (2010a), "Out-of-plane strengthening of unreinforced masonry walls using near surface mounted fibre reinforced polymer strips", *J. Struct. Eng. Soc. NZ. Inc.*, **23**(2), 91-103.
- Dizhur, D., Derakhshan, H., Lumantarna, R. and Ingham, J.M. (2010b), "In-situ out-of-plane testing of unreinforced masonry wall segment in Wintec Block F building", *2010 New Zealand Society for Earthquake Engineering Technical Conference*, Wellington, New Zealand.
- Dizhur, D., Lumantarna, R., Derakhshan, H. and Ingham, J.M. (2010c), "In-situ testing of a residential unreinforced masonry building in Wellington, New Zealand", *8th International Masonry Conference*, Dresden, Germany.
- Durham, A.S. (2002), "Influence of confinement plates on the seismic performance of reinforced clay brick masonry walls", M.Sc. Thesis, North Carolina State University, Raleigh, North Carolina, USA.
- Ehsani, M., Saadatmanesh, H. and Velazquez-Dimas, J. (1999), "Behavior of retrofitted URM walls under simulated earthquake loading", *J. Compos. Constr.*, **3**(3), 134-142.
- Erdal, M. (2010), "Improving out-of-plane strength and ductility of unreinforced masonry walls in low-rise buildings by centrally applied FRP strip", *Int. J. Phys. Sci.*, **5**(2), 116-131.
- Ghobarah, A. and El Mandooh Galal K. (2004), "Out-of-plane strengthening of unreinforced masonry walls with openings", *J. Compos. Constr.*, **8**(4), 298-305.
- Haddad, M.A., Shaheen, E., Parsekian, G.A., Tilleman, D. and Shrive, N.G. (2010), "Strengthening of a concrete masonry wall subject to lateral load with sprayed glass-fibre-reinforced polymer", *Can J. Civ. Eng.*, **37**(10), 1315-1330.
- Hamilton III H.R. and Dolan, C. (2001), "Flexural capacity of glass FRP strengthened concrete masonry walls", *J. Compos. Constr.*, **5**(3), 170-178.
- Hamoush, S.A., McGinley, M.W., Mlakar, P., Scott, D. and Kenneth, M. (2001), "Out-of-plane strengthening of masonry walls with reinforced composites", *J. Compos. Constr.*, **5**(3), 139-145.
- Ismail, N., Laursen, P.T., Schultz, A.E. and Ingham, J. M. (2011), "Cyclic out-of-plane behaviour of post-tensioned clay brick masonry", *The Eleventh North American Masonry Conference*, Minneapolis, Minnesota, USA.
- Kanit, R. and Atimtay, E. (2006), "Experimental assessment of the seismic behavior of load-bearing masonry walls loaded out-of-plane", *Turkish J. Eng. Envir. Sci.*, **30**(2), 101-113.
- Papanicolaou, C., Triantafillou, T. and Lekka, M. (2011), "Externally bonded grids as strengthening and seismic retrofitting materials of masonry panels", *Constr. Build. Mater.*, **25**(2), 504-514.
- Prota, A., Marcari, G., Fabbrocino, G., Manfredi, G. and Aldea, C. (2006), "Experimental in-plane behavior of tuff masonry strengthened with cementitious matrix-grid composites", *J. Compos. Constr.*, **10**(3), 91-103.

TEC-2007 Turkish Earthquake Code (2007), *Regulations on Structures Constructed in Disaster Regions*, Ministry of Public Works and Settlement, Ankara, Turkey.  
Turkish Standard TS 498 (1997), *Design Loads for Buildings*, Turkish Standards Institutions, Ankara, Turkey.

CC